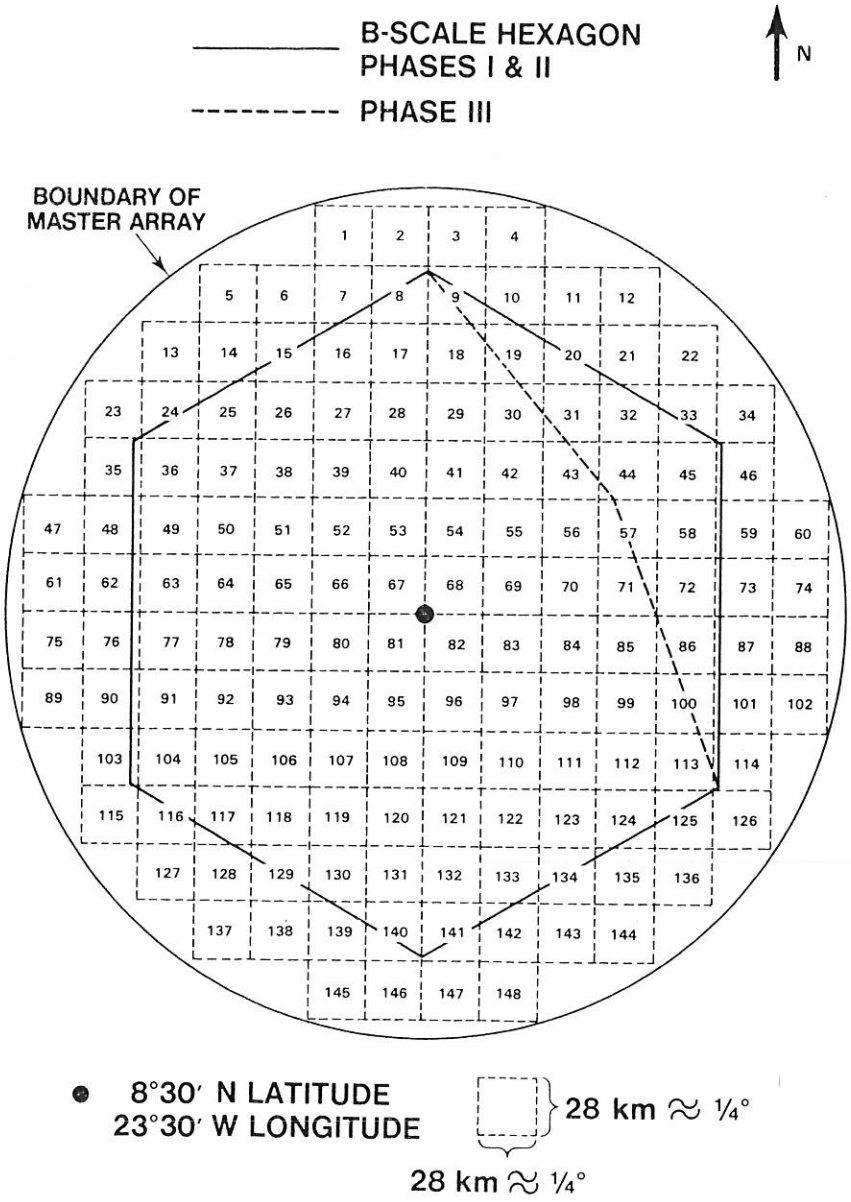

Figure 3.--Schematic of latitude-longitude network within master array, which is centered on hexagonal B-scale ship array.

2. INPUT DATA USED TO DERIVE RAINFALL PRODUCTS

The input data used in the derivation of the atlas products are those contained in data set No. 4.36.02.104 (table 1). A sample graphics display of these data is shown in figure 2.

The input rainfall values were obtained by merging the refined rainfall estimates, within the master array, from two or more of the individual radars. The precipitation processing and merging procedures for Phases I and II were considerably different from Phase III. For Phases I and II, only data from the Oceanographer and Researcher radars were used in the derivation of the hourly maps (fig. 4); for Phase III, data from all four C-band radars were merged when available (fig. 5).

The decision to use only NOAA radar data for Phases I and II was based largely on considerations of data availability and on the fact that the Oceanographer radar covered the complete master array during the first two Phases, when the Oceanographer was stationed near the center of the array. Because the Oceanographer radar data alone were fundamental to the accuracy of the Phase I and II estimates, major efforts were undertaken to refine these data by applying atmospheric, wet radome, and intervening rainfall attenuation corrections. For Phase III, only atmospheric attenuation corrections were applied to the radar data from the four C-band radars. Rainfall attenuation corrections were not considered as significant for Phase III, because data were merged from more radars, each of which viewed the precipitation lying in the interior of the array from different directions (fig. 5). Intervening rainfall attenuation was normally not significant at C-band frequencies for GATE convection, except for very small localized areas (Patterson et al., 1979).

The method used for merging the data from the multiple radars also was different for Phase III; namely, the nonzero rainfall amounts, for the common data bins falling inside the master array from the various radars, were averaged. For Phases I and II, all nonzero rainfall rates from the Oceanographer radar were taken alone as the best estimates. Nonzero estimates from the Researcher radar were substituted only for common data bins within the master array where the Oceanographer values were zero. During Phases I and II, this merging technique recovered data that were sometimes missed by the Oceanographer radar because of an obstruction of the radar beam by the ship's superstructure in a sector, about 20° wide, forward of the ship. The Oceanographer's obstructed sector was normally located in areas covered by the Researcher radar.

The scope here has been confined to a brief description of the rainfall processing system, which prepared the input data used in the derivation of the atlas products. A more complete description of the processing is given by Patterson et al. (1979).

3. RAINFALL STATISTICS

The rainfall statistics presented in this section have been included to provide background information on the rain-rate regime observed during GATE. They should help in the interpretation of the GATE rainfall data relative to rainfall regimes in other parts of the world. These statistics, which should be of particular interest to hydrometeorologists and communication engineers, are only examples of the types of rainfall statistics that may be derived

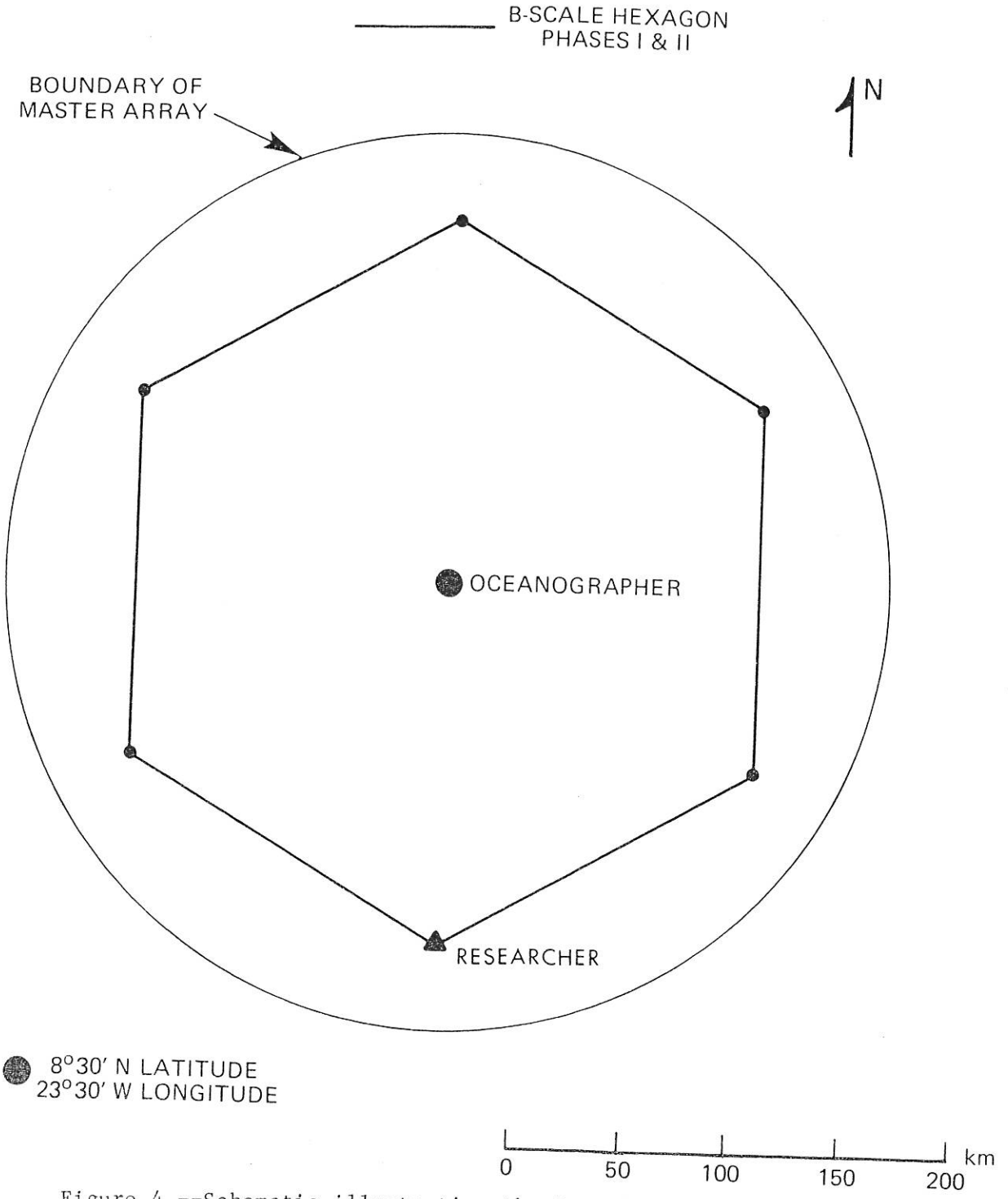

Figure 4.--Schematic illustrating the B-scale and master arrays and location of C-band radars used in rainfall derivations for Phases I and II of GATE.

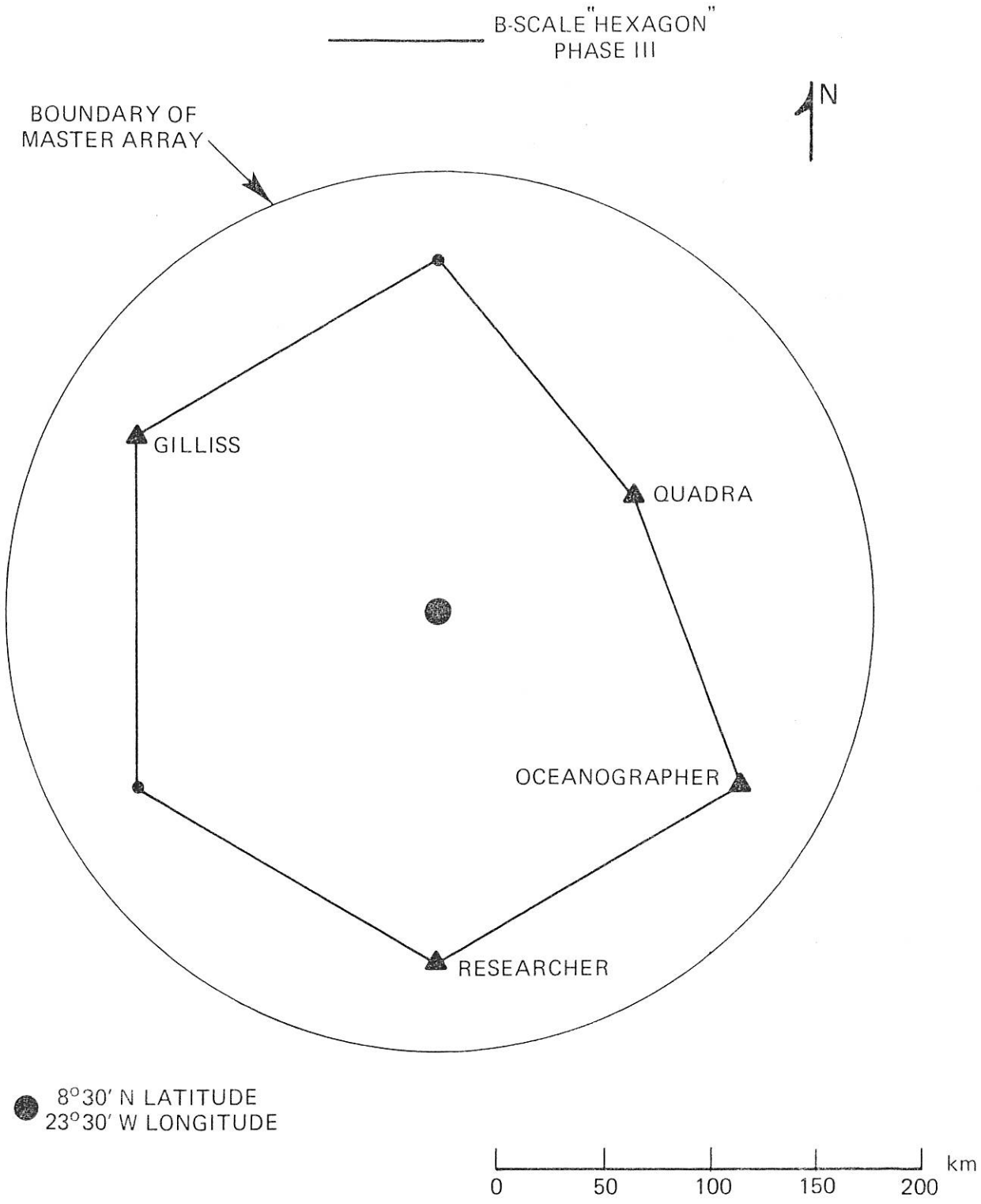

Figure 5.--Schematic illustrating B-scale and master arrays and the location of C-band radars used in rainfall derivations for Phase III of GATE.

from the variety of rainfall data sets now available from the GATE archives (sec. 1.2). Furthermore, analogous statistics for other time scales and larger space scales can be derived directly from the rainfall data contained in this atlas.

3.1 Rainfall-Rate Frequency Distributions for Selected Durations

Cumulative frequency distributions of rainfall rate are presented in figure 6 for selected durations and areas. The radar data and the analysis regions used to composite the statistics for these frequency distributions are summarized in table 2. The cumulative curves give the percent of the rates that are less than a given ordinate value and that exceed a specified threshold. The thresholds for the curves labeled as instantaneous 16 km^2, hourly 16 km^2, daily 16 km^2, and hourly 784 km^2 are 1.2 mm hr^{-1}, 0.5 mm hr^{-1}, 0.02 mm hr^{-1}, and 0.01 mm hr^{-1}, respectively.

The instantaneous frequency distribution emphasizes that the intense convective rainfall cores observed in GATE were confined to a very small fraction of the total rain area. The distribution of rates becomes more uniform for the larger spatial and/or temporal averaging scales. The distributions for the hourly 784-km^2 and the daily 16-km^2 scales are very similar, indicating that some degree of ergodicity is reached for these combinations of space and time scales.

3.2 Maximum Point Rainfall for Various Durations

Figure 7 presents plots of maximum point rainfall accumulations for the range of durations sampled during GATE. For the radar curve, 4-km x 4-km data bins are treated as "point" values. The data used for the radar analysis were the merged rainfall estimates from the C-band radars (sec. 2). The analysis region, used in the determination of the maximum rainfall accumulations from radar, was the total master array. Because the absolute maxima occurred outside the subareas of the master array used in the derivation of the frequency distributions shown in figure 6, the maximum values given on the 4-km curves in figure 6 are somewhat lower than the corresponding values on the radar curve in figure 7.

All shipboard rain-gage data contained in the reports by Seguin and Sabol (1976) and Seguin and Crayton (1977) were examined, and the absolute maxima of all gage values for the various durations were selected for the gage plot shown in figure 7. For all durations of Phase length ($\simeq$ 20 days) and less, a rain gage aboard the Oceanographer caught the largest gage amounts. The largest cumulative gage value for all three GATE Phases combined ($\simeq$ 60 days) was collected by a rain gage aboard the Researcher.

The Julian days that the maxima occurred, for durations up to daily, appear beside the plotted points on both the radar and shipboard gage curves. A cross-reference between Julian day and the month and day can be made by referring to the headers accompanying the tabulated rainfall data for each day.

A World Record Curve from Chow (1964) is also included in figure 7 for comparison with the GATE radar and rain-gage curves. The values for the GATE curves are based on specific beginning and ending times; for example, the

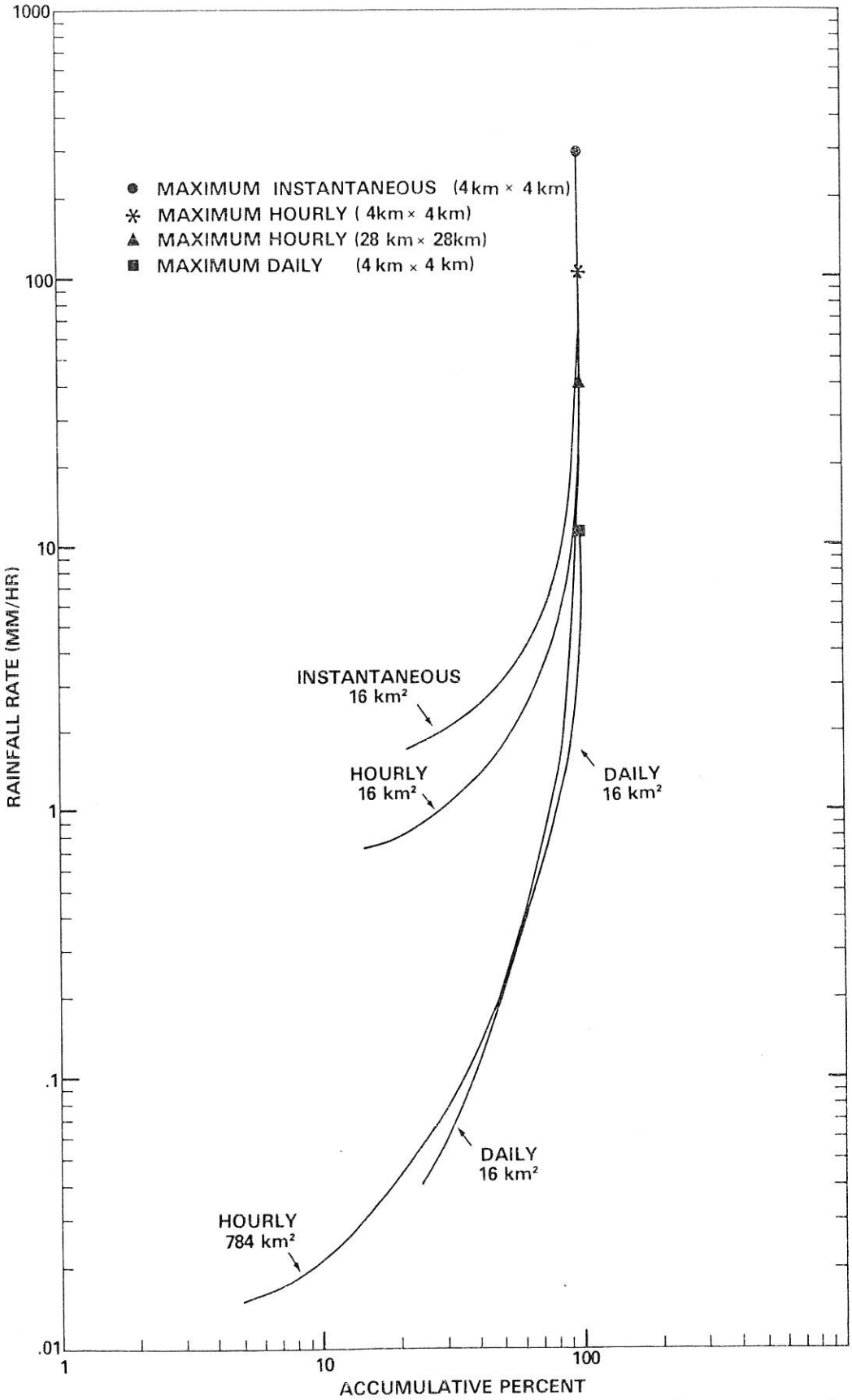

Figure 6.--Cumulative frequency distributions of average rainfall rates for selected spatial and temporal averaging scales (areas and durations), derived from GATE radar measurements specified in table 2. Maximum rainfall rate for each distribution is indicated with special symbol.

Table 2.--Radar data sets, analysis periods, and analysis regions used in the derivation of the rain-rate frequency distributions given in figure 6

Averaging Scales		Data Set No. (see table 1)	Analysis Period	Analysis Region
Time	Space			
Instantaneous	4 km x 4 km	3.36.02.103 3.36.02.106 With bias and atmospheric attenuation corrections added	First 9½ days of Phase III data from Oceanographer radar and all Phase III data from Gilliss radar	Two 8000-km^2 boxes for Oceanographer data and one 8000-km^2 box for Gilliss data, located within optimum ranges of the respective radar.
Hourly	4 km x 4 km	4.36.02.104	Phases I, II, III	160-km x 160-km box centered within master array
Hourly	28 km x 28 km ≈ ¼° x ¼°	4.36.02.106	Phases I, II, III	160-km x 160-km box centered within master array
Daily	4 km x 4 km	4.36.02.104	Phases I, II, III	160-km x 160-km box centered within master array

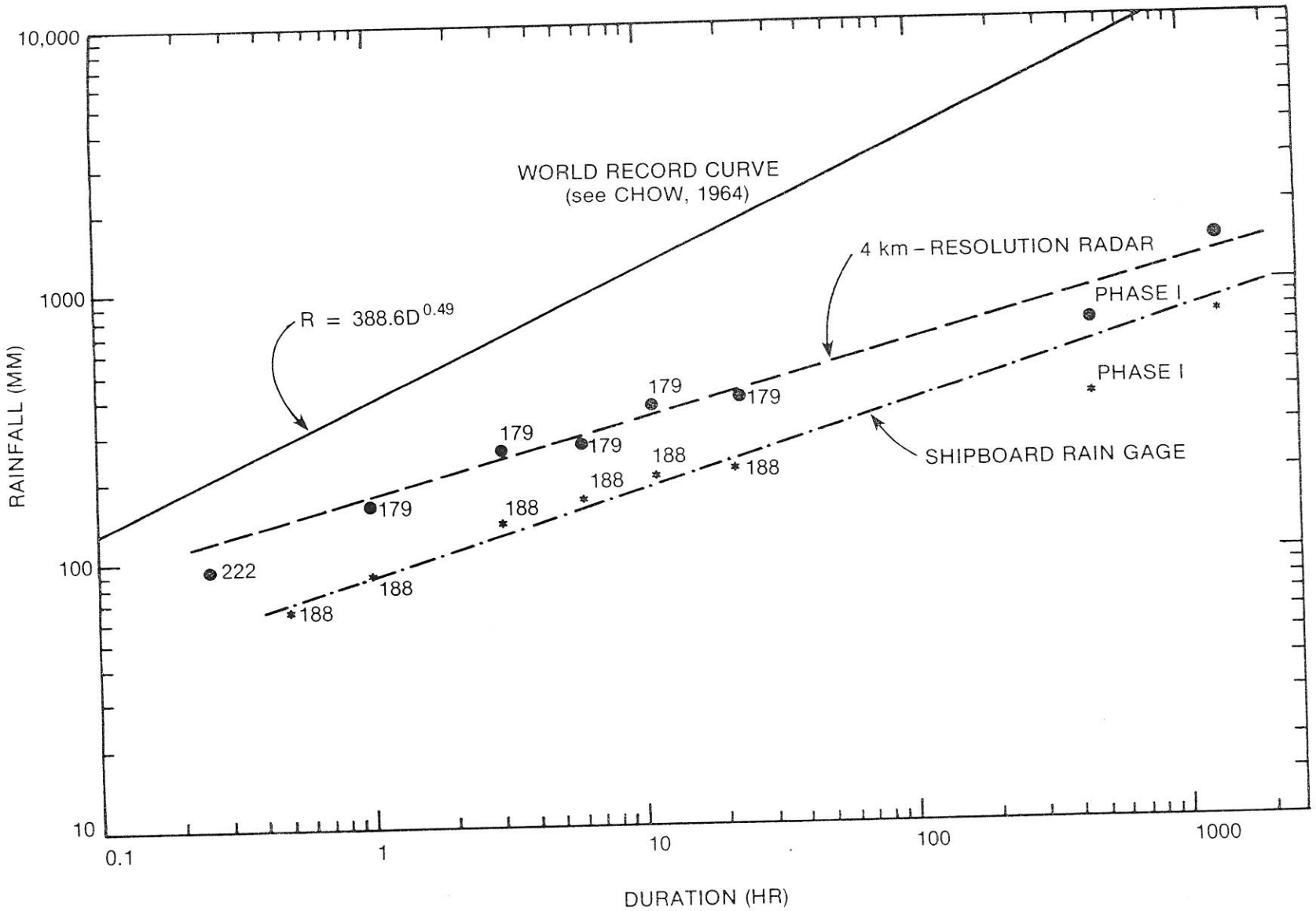

Figure 7.--Plots of maximum point rainfall accumulations observed during GATE for specific end times and various durations and an analogous curve for variable end times based on world record events.

daily accumulations used in the analyses were for 24-hr periods ending at midnight GMT, and the 12-hr accumulations were for periods ending at 1200 GMT and 2400 GMT, and so forth, for the other durations. The World Record Curve is based on the absolute maximum accumulations that have been recorded anywhere in the world for given durations, irrespective of the beginning and corresponding ending times. All values for the World Record Curve are from land stations where terrain features, such as orographic lifting, are often important.

Some interesting observations can be made by comparing the curves in figure 7. First, the GATE radar maxima are consistently higher than those recorded by the shipboard rain gages, although the two curves become closer as the duration increases. This difference is not because of a calibration problem with either sensor but primarily results from incomplete spatial sampling by the widely spaced rain-gage observations. The radar and gage maxima converge for longer durations as the mean rainfall fields become more uniform, increasing the probability that a gage will record a value closer to the absolute maximum. However, the rainfall distribution for the three Phases combined was still sufficiently skewed that no gage caught the absolute maximum.

It is also interesting to note that the radar curve and the World Record Curve approach each other for the shorter durations. This is physically consistent with the fact that some of the GATE systems produced quite intense rainfall for relatively short durations, but the convective and transitory nature of the GATE storms precluded extremely large accumulations at a point for the longer durations.

4. DESCRIPTION OF RAINFALL ESTIMATES

4.1 Missing Data and Derivation of Mean Rates

Except for the 69 consecutive hours that were missed during Phase II when the Oceanographer was off station for a medical evacuation, gaps in the rainfall record are confined to infrequent periods of only a few hours in duration. The hours for which rainfall estimates are missing on a given day appear in the header of the isohyetal map for that day. Also, blank lines in the hourly section of the rainfall tables indicate missing rainfall rates for those hours.

The estimates of mean rainfall rate for the 3-, 6-, 12-, and 24-hr periods were obtained by first summing the nonmissing hourly rates and then dividing the totals by the number of hours within the period that data were available. Mean rates were not calculated when more than one-third of the hourly values within the period were missing. This method of calculation gives "exact" mean rates for the portion of the period covered by existing hours. How representative these mean rates are for the total period depends on the length of the data gap(s) and on whether the mean patterns during the missing hour(s) differed significantly from those observed during the existing hours. The specific hours missing from a period can be identified as previously described.

4.2 Time Series and Array Means for Three GATE Phases

With the exception of the Phase mean rates for the A/B-scale hexagon,[2] which were obtained by extrapolating the B-scale radar estimates using infrared satellite data, the rainfall rates given in this section were derived from the data given in the rainfall tables. The Phase mean values, combined with the B-scale time series, provide a summary of the average precipitation production rates and their temporal distribution.

Figure 8 gives time series of 6-hr mean rainfall rates over the B-scale array for the three Phases of GATE. As can be inferred from figure 8, synoptic scale events, occurring at an average frequency of about once each 3.5 days, affected the precipitation production in the B-scale. Reed et al. (1977) and Hudlow (1977) have shown, for Phase III data, that the precipitating convection was significantly enhanced in the vicinity of the troughs of African waves, which were identified on 700-mb wind charts.

The Phase mean rainfall-rate estimates for the B- and A/B-scale arrays are given in table 3. The A/B-scale estimates, which are included because of their importance in A/B-scale budget analyses, were obtained by extrapolating the B-scale radar estimates using satellite data as follows:

$$(\overline{\text{Rain}})_{AB} = \left[(\overline{\text{High Cloud}})_{AB} \Big/ (\overline{\text{High Cloud}})_{B}\right] \times (\overline{\text{Radar Rain}})_{B} ,$$

where the bars indicate Phase mean values over the arrays as indicated by the subscripts. The high cloud was determined from infrared satellite data collected from the Synchronous Meteorological Satellite-1 (SMS-1). High cloud was defined as the average percent area covered by cloud image exceeding an altitude of 7.8 km (25 k ft), which corresponds to a brightness temperature threshold of approximately -20°C for the GATE area. This threshold closely corresponds to the one that Stout et al. (1977) found to give the best correlations between infrared image area and observed rainfall as measured by radar.

The validity of using the radar/satellite extrapolation technique can be evaluated by examining the correspondence between the relative variations of the radar and the satellite B-scale values for the three Phases. Comparison of the B-array columns in table 3 shows that the relative variations from Phase to Phase closely agree. While this method of extrapolating appears to work well for Phase averages, its validity would probably diminish for much shorter periods. However, using considerably more sophisticated procedures, 6-hourly rainfall estimates covering an A-scale array, which includes the A/B scale, have been derived from SMS-1 data by Griffith et al. (1979). These satellite rainfall estimates are available on magnetic tape from the GATE World Data Center A (1978; see data set No. 5.89.02.102 in the GATE Data Catalogue).

It should be noted that the estimates of mean rainfall rate for Phase II (table 3) are based on only the 16 days with existing radar data. However, the satellite mean high-cloud values also were computed including the 3 days missed by the radar, and these values were virtually identical to the ones given in

---

[2]The A/B-scale hexagon is centered on, and symmetric with, the B-scale hexagon, but it covers an area 5 times larger (Kuettner et al., 1974). Accordingly, it is 2.7 times larger than the master array (fig. 4).

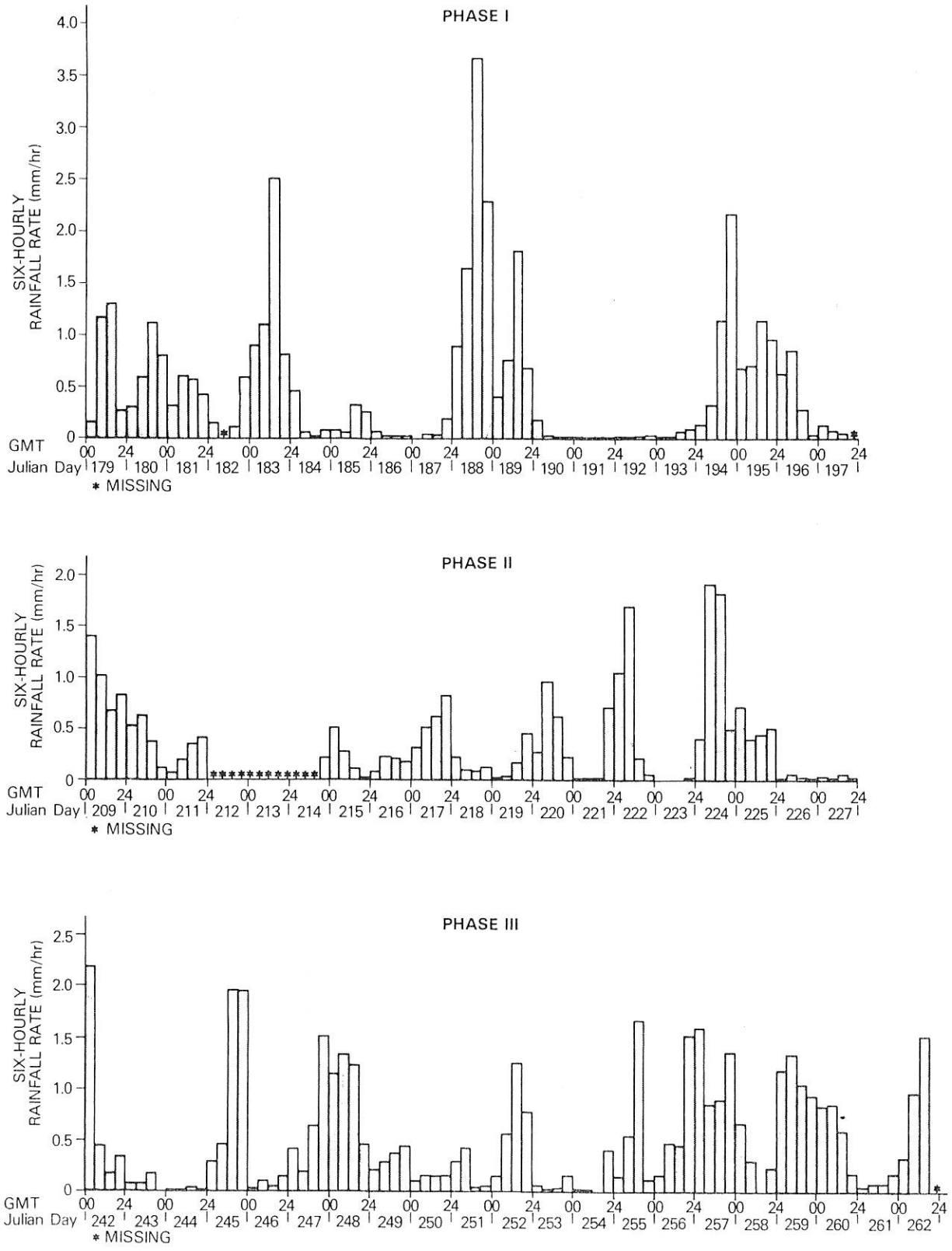

Figure 8.--Time series of 6-hourly average rainfall rate over B-scale hexagon, derived from C-band radar measurements.

Table 3.--Estimates of the Phase mean rainfall rates (mm day^{-1}) and percent satellite high-cloud coverages over the B- and A/B-scale arrays

	B-Array		A/B-Array	
Phase	Radar rain rate	Satellite percent high-cloud cover	Satellite percent high-cloud cover	Extrapolated radar rain rate via satellite ratio
I	11.9	21	19	10.8
II	9.2	15	14	8.6
III	12.7	25	22	11.2
Average all Phases	11.3 mm/day	20.3%	18.3%	10.2 mm/day

table 3 without the 3 days. This supports the conclusion that the B-array mean radar estimate for Phase II was not seriously degraded because of the three days of missing data.

Finally, we emphasize that although the A/B-scale rain estimates may be subject to greater uncertainty than those for the B-scale, they are almost certainly superior to estimates determined from only the shipboard rain gages. It is probable that the widely spaced rain-gage observations will underestimate the true array means, because of the skewed distribution of the Phase rainfall patterns.

4.3 Format of Rainfall Products

The rainfall products are arranged chronologically with the mean isohyetal map for each Phase preceding the series of daily maps and tables for the Phase. All rainfall values are expressed as average rainfall rates (mm hr^{-1}), over the area and period to which they pertain, and all times are Greenwich mean time (GMT). Accumulations can be obtained for a particular period by multiplying the rates times the number of hours in the period.

The number of digits carried past the decimal point should not be taken as an indication of the absolute accuracy of the rain-rate estimates. More decimal places were retained than in some cases are warranted by the accuracy of the measurements, so that the difference between zero and very small rain amounts can be distinguished. This becomes increasingly important as the period and/or area over which the rainfall estimates are being averaged increase. For example, a moderately intense, but brief and isolated, shower may result in a very small mean rainfall rate when averaged over the total B-array for a 24-hr period.

4.3.1 Phase Isohyetal Maps

The contours on each Phase map were manually drawn from an array of Phase mean rainfall-rate values. The elements of the array were obtained by spatially averaging the 4-km resolution data over 16-km x 16-km squares.

Also plotted on the Phase isohyetal charts are the mean rainfall rates calculated from the shipboard rain-gage catches for ship stations in the B-scale array. The letter following the rain-rate value denotes the approximate location of the gage aboard the ship. Data were available from two or more gages for some ships. For these cases, the (maximum) deviation between the value for the plotted gage and the other gage(s) is shown in parenthesis. The triangles mark the navigated gage positions, which are averages calculated by weighting the mean hourly ship positions by the hourly rainfall amounts. In most cases the difference between the rain weighted position and the straight average position is small, and the gage-to-radar correspondence is not affected significantly. There are some notable exceptions; for example, the Oceanographer for Phase I.

4.3.2 Daily Isohyetal Maps

The daily isohyetal displays consist of graphics images, composed of 4-km x 4-km data bins, generated from a set of 16 alphanumeric characters, which provides an intensity resolution of 1.75 decibels. Four gray shades indicating successively higher rainfall rates are illustrated by increasing the number of dots (pixels) used to form the characters.

The key relating the alphanumeric characters to the daily-mean rain rates is given in the header. Hours for which data are missing (see sec. 4.1) are also listed in the header. Finally, the number of scans (maps) of instantaneous data that were used from each radar to derive the hourly data, which in turn were used to derive the daily map, are given in the map header. The maximum possible number of scans that can appear in the header for a given radar and day is 120, which indicates that all of the instantaneous scans, collected at 15-min intervals, were available. The trapezoidal integration algorithm used all of the "on-the-hour" scans twice, and they were likewise included twice in the header count.

4.3.3 Tabulated Mean Rainfall Rates for Various Durations and Geometric Areas

Fifteen area numbers appear across the top of each rainfall table, and the ending hours for the various periods appear down the left side of the table. The 15 area numbers correspond to the 15 geometric areas shown in figure 9. The assigned ship positions shown in table 4 were assumed in determining the boundaries for all computations.

The values contained in the tables give the radar estimates of the average rainfall rates over the various geometric areas and over the 1-, 3-, 6-, 12-, and 24-hr periods within each day. For example, the average rainfall rates (mm hr^{-1}) over the B-scale hexagon (area No. 9) on Julian day 179 (June 28) for the first time period in each duration category, i.e., over hours 00-01, 00-03, 00-06, 00-12, and 00-24, are 0.27, 0.21, 0.15, 0.67, and 0.75, respectively.

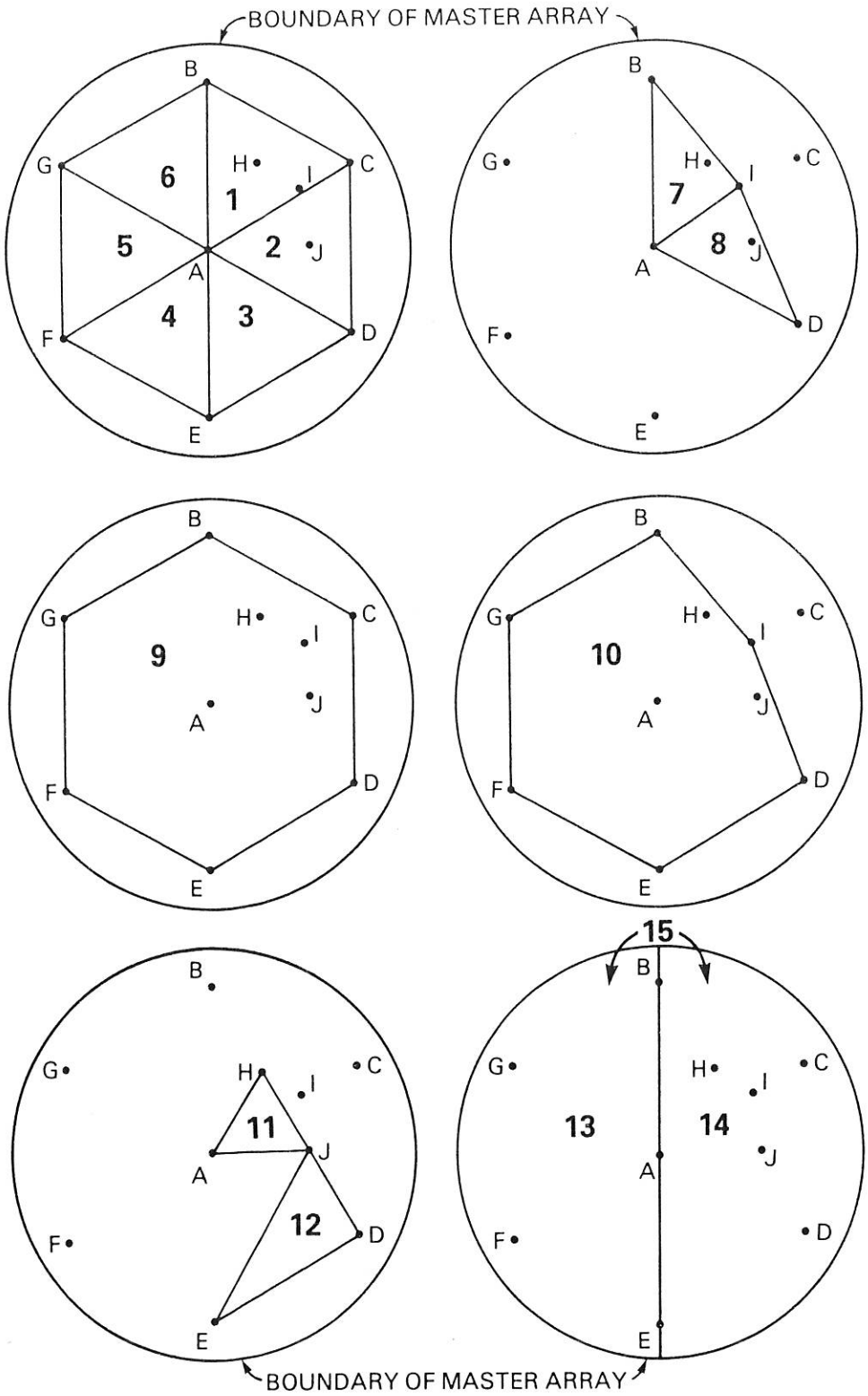

Figure 9.--Key giving geometric areas corresponding to the area numbers appearing above the columns of the daily rainfall tabulations. Letters designate ship positions.

Table 4.--Assigned ship positions used in determining the boundaries of the geometric areas shown in figure 9

Ship position	Latitude (N)	Longitude (W)
A	8°30'	23°30'
B	10°00'	23°30'
C	9°15'	22°12'
D	7°45'	22°12'
E	7°00'	23°30'
F	7°45'	24°48'
G	9°15'	24°48'
H	9°15'	23°05'
I	9°00'	22°40'
J	8°30'	22°38'

4.4 Expected Accuracies of Rainfall Estimates

4.4.1 Background

Because of the large spatial and temporal gradients, it is always difficult to establish the absolute accuracy of convective rainfall measurements, even over land areas. At sea it becomes more difficult, since adequate independent "ground truth" measurements are usually not available, especially for the smaller space and shorter time scales. Most radar hydrologists accept that comparisons made against a dense rain-gage network, within optimum range of a land-based radar, often provide the best information for assessing the accuracy of, and for calibrating, radar rainfall estimates. However, it would not have been logistically feasible, if possible, at all, to erect and maintain a dense network of buoys, instrumented with rain gages, in the GATE B-scale area.

Since it was clear early in the planning of the GATE radar program that a dense network of gages would not be available, and that the success of the water and energy budget studies would critically depend on the accuracy of the quantitative radar estimates, a multi-faceted approach for calibrating and intercomparing the data from the four C-band radar systems was undertaken (Hudlow et al., 1979). The electronic calibrations were established before the GATE field Phases and were routinely checked throughout the summer of 1974. A major subtask of the post analyses was the evaluation of the radar calibrations through a variety of intercomparison analyses, which included comparisons of radar measurements from two or more radars in regions of overlapping coverage, and comparisons of the rainfall estimates from the individual radars with rain-gage measurements collected aboard the B-scale ships (figs. 4 and 5). Based on these intercomparisons, systematic biases were estimated, and adjustments for them were made as a part of the derivation of the final rainfall estimates (Patterson et al., 1979).

In arriving at the magnitudes of the systematic biases, considerable weight was given to the comparisons between the Phase rainfall totals from the